

# CRISPR/Cas9-mediated generation and analysis of N terminus polymorphic models of $\beta_2$ AR in isogenic hPSC-derived cardiomyocytes

Alexander Kondrashov,<sup>1,3</sup> Nurul A.N. Mohd Yusof,<sup>1,5</sup> Alveera Hasan,<sup>2</sup> Joëlle Goulding,<sup>3,4</sup> Thusharika Kodagoda,<sup>2</sup> Duc M. Hoang,<sup>1,6</sup> Nguyen T.N. Vo,<sup>1</sup> Tony Melarangi,<sup>1</sup> Nazanin Dolatshad,<sup>2</sup> Julia Gorelik,<sup>2</sup> Stephen J. Hill,<sup>3,4</sup> Sian E. Harding,<sup>2</sup> and Chris Denning<sup>1</sup>

<sup>1</sup>Division of Cancer and Stem Cells, University of Nottingham Biodiscovery Institute, University Park, Nottingham NG7 2RD, UK; <sup>2</sup>National Heart and Lung Institute, Imperial College, London W12 0NN, UK; <sup>3</sup>Centre of Membrane Proteins and Receptors (COMPARE), Universities of Birmingham and Nottingham, Midlands, UK; <sup>4</sup>Division of Physiology, Pharmacology and Neuroscience, School of Life Sciences, University of Nottingham, Nottingham, UK

During normal- and patho-physiological situations, the behavior of the beta2-adrenoreceptor ( $\beta_2$ AR) is influenced by polymorphic variants. The functional impact of such polymorphisms has been suggested from data derived from genetic association studies, *in vitro* experiments with primary cells, and transgenic overexpression models. However, heterogeneous genetic background and non-physiological transgene expression levels confound interpretation, leading to conflicting mechanistic conclusions. To overcome these limitations, we used CRISPR/Cas9 gene editing technology in human pluripotent stem cells (hPSCs) to create a unique suite of four isogenic homozygous variants at amino acid positions 16(G/R) and 27(G/Q), which reside in the N terminus of the  $\beta_2$ AR. By producing cardiomyocytes from these hPSC lines, we determined that at a functional level  $\beta_2$ AR signaling dominated over  $\beta_1$ AR. Examining changes in beat rates and responses to isoprenaline, Gi coupling, cyclic AMP (cAMP) production, downregulation, and desensitization indicated that responses were often heightened for the GE variant, implying differential dominance of both polymorphic location and amino acid substitution. This finding was corroborated, since GE showed hypersensitivity to doxorubicin-induced cardiotoxicity relative to GQ and RQ variants. Thus, understanding the effect of  $\beta_2$ AR polymorphisms on cardiac response to anticancer therapy may provide a route for personalized medicine and facilitate immediate clinical impact.

## INTRODUCTION

The beta-adrenergic receptors ( $\beta$ ARs) are members of the G-protein-coupled receptor (GPCR) superfamily. They have important roles in various diseases, including cardiovascular disease and asthma, hence are common protein targets for therapeutic intervention.<sup>1,2</sup> While there are 3  $\beta$ ARs ( $\beta_1$ AR,  $\beta_2$ AR, and  $\beta_3$ AR),  $\beta_3$ AR is not cyclic AMP (cAMP)-dependent, and its role in acute contractile changes is unclear. In cardiomyocytes, both  $\beta_1$  and  $\beta_2$  receptors are often found together but are spatially separated and co-localized with different

effector complexes.<sup>3,4</sup> Thus, both  $\beta_1$ AR and  $\beta_2$ AR receptors can be coupled to adenylate cyclase through the Gs subunit of trimeric G-protein. However, only  $\beta_2$ AR can activate an alternative Gi-mediated pathway.<sup>5,6</sup> This alternative coupling means  $\beta_2$ AR can counteract proapoptotic signaling mediated by  $\beta_1$ AR<sup>7</sup> after prolonged catecholamine stimulation, and hence the  $\beta_2$ AR variant is often considered as cardioprotective.<sup>8</sup>

Multiple single-nucleotide polymorphisms exist in *ADRB2*, the gene that encodes  $\beta_2$ AR.<sup>9</sup> Two of the most common variants cause nonsynonymous substitutions at positions of 16 (Gly to Arg; G to R) and 27 (Glu to Gln; E to Q) in the N terminus of  $\beta_2$ AR.

Numerous genetic association studies have suggested that these variants may modulate the risk of developing heart failure, asthma and airway hyper-responsiveness, protection from traumatic or septic shock, obesity, and cancer, where  $\beta_2$ AR plays a central role.<sup>10–14</sup> Nevertheless, data often lead to conflicting mechanistic explanations, likely relating to the complex and heterogenic nature of the *ADRB2* locus.<sup>15,16</sup>

The impact of the polymorphisms in modulating functional responses of  $\beta_2$ AR to stimulation with agonists has also been

---

Received 4 May 2020; accepted 20 October 2020;  
<https://doi.org/10.1016/j.omtm.2020.10.019>.

<sup>5</sup>Present address: Institute for Medical Research, Block C, National Institutes of Health (NIH) Malaysia, No 1, Jalan Setia Murni U13/52, Seksyen U13, Setia Alam, 40140 Shah Alam, Selangor, Malaysia.

<sup>6</sup>Present address: Department of Cellular Manufacturing, Vinmec Research Institute of Stem Cell and Gene Technology, Hanoi, Vietnam

**Correspondence:** Chris Denning, Division of Cancer and Stem Cells, University of Nottingham Biodiscovery Institute, University Park, Nottingham NG7 2RD, UK.  
**E-mail:** [chris.denning@exmail.nottingham.ac.uk](mailto:chris.denning@exmail.nottingham.ac.uk)

**Correspondence:** Alexander Kondrashov, Division of Cancer and Stem Cells, University of Nottingham Biodiscovery Institute, University Park, Nottingham NG7 2RD, UK.  
**E-mail:** [a.kondrashov@nottingham.ac.uk](mailto:a.kondrashov@nottingham.ac.uk)



investigated. To this end, the approaches employed include using primary cell lines derived from genotyped individuals, such as lymphoblasts or airway smooth muscle cells,<sup>17,18</sup> and stable or transient receptor overexpression in HEK293 or Chinese hamster ovary (CHO) immortalized lines.<sup>19,20</sup> Although the polymorphic variants caused changes such as agonist-promoted receptor desensitization and downregulation,<sup>19</sup> and trafficking in cytoplasm and phosphorylation pattern of the  $\beta_2$ AR,<sup>20,21</sup> the results were not always in concordance with each other.<sup>19,20</sup> These model systems are limited by the high level of transgene expression and/or variability in the background genotype, factors known to cause phenotypic variability that exceeds the impact of the polymorphic modification.<sup>22,23</sup> This has led to the notion that the gold standard is to engineer isogenic sets of cell lines, wherein only the polymorphism of interest is changed within an otherwise constant genetic background.

In the current study, we present and functionally characterize a unique set of homozygous isogenic human pluripotent stem cell (hPSC) lines and derived cardiomyocytes carrying four  $\beta_2$ AR N-terminal polymorphic combinations at positions 16 and 27, namely Gly16-Glu27 (GE), Gly16-Gln27 (GQ), Arg16-Gln27 (RQ), and Arg16-Glu27 (RE).

## RESULTS

### Engineering of isogenic hPSC lines carrying GE, GQ, RQ, and RE variants in the $\beta_2$ AR

To study the influence of polymorphisms on cardiomyocyte function, we created 4 isogenic homozygous variants within HUES7, a human embryonic stem cell (hESC) line,<sup>24</sup> at positions 16 and 27 of the  $\beta_2$ AR protein (46 and 79 of the *ADRB2* coding sequence). This entailed coupling CRISPR/Cas9 and *PiggyBac* approaches in a two-step “in-out” seamless strategy, which we recently published<sup>22</sup> (Figure 1A). Targeting vectors contained the polymorphic variants within the left arm of homology, while a puromycin<sup>+</sup> selection cassette was flanked by *PiggyBac* transposon terminal repeats (Figure 1A; Figure S1A).

The targeting process in hPSCs followed sequential steps: transfection with vectors and selection using puromycin to isolate drug-resistant clones (the “in” step; Figure S1B), which were then transfected with transposase to excise the selection cassette via recombination of *PiggyBac* sequences, thus reconstituting the locus and rendering the cells insensitive to ganciclovir (the “out” step; Figure S1B). The use of *PiggyBac* transposon targeting vector requires the presence of the TTAA integration/excision sequence. Since the nearest TTAA sequence to polymorphic positions exceeded the limit of efficient gene conversion (748 bases away from gRNA-A1 cleavage site; Figure S1A), we used codon redundancy to make a synonymous change in Leu42-Ile43 (CTCATC to TTAATC) (Figure 1A; Figure S1A).

Clones for the four  $\beta_2$ AR variants (GE, GQ, RQ, and RE) were verified by PCR genotyping, and “scar-free” fidelity of the locus after *PiggyBac* cassette excision was confirmed by sequencing (Figures S1C and S1E). It was important to discount the possibility of multiplications of tar-

geted sequences and of large deletions in the second allele, which has been reported by others<sup>25</sup> and can cause allelic dropout in PCR screening approaches. qPCR analysis showed similar values between the variants (Figure S2E). In addition, we exploited the suboptimal excision properties of transposase to demonstrate that both alleles could be detected by PCR in clones where excision of *PiggyBac* had only occurred in one allele, hence giving a size differential (Figure S3).

We also used primers designed to detect vector elements to ensure random sequences were not integrated elsewhere in the genome (Figures S1F and S2E). qPCR with targeting vector-specific primers did not detect the presence of randomly integrated plasmids into the genome of these isogenic cell lines (Figure S1D). This confirmed cassette excision and seamless restoration of the *ADRB2* locus, concurrent with incorporation of the different polymorphisms within the HUES7 genetic background, thereby providing a resource for characterization, cardiomyocyte differentiation, and phenotypic analysis.

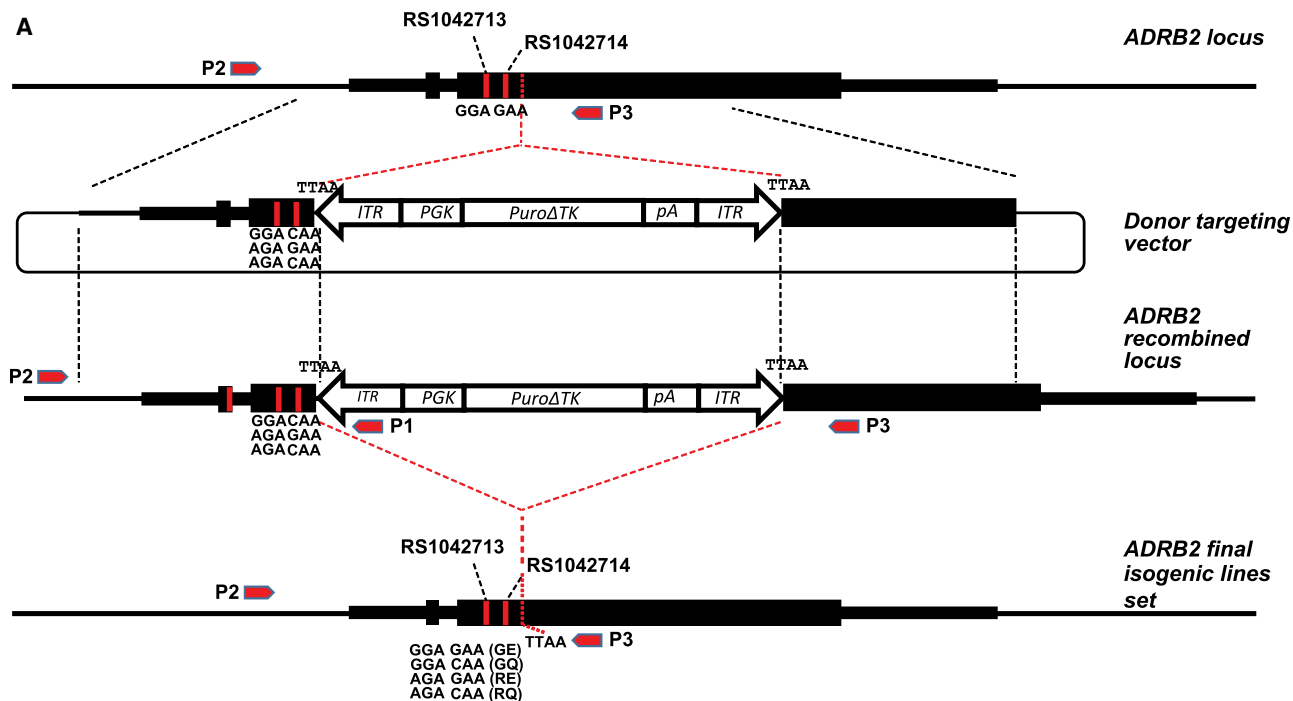
### Characterization of isogenic $\beta_2$ AR variant lines

The isogenic lines displayed properties consistent with pluripotency relating to high nuclear to cytoplasmic ratio; compacted morphology; expression of OCT4, NANOG, and SOX2 markers; normal 46, XY chromosome complement; and constant proliferation through serial passages (Figures S2A–S2D). Directed differentiation as monolayers, via a protocol we published previously,<sup>22</sup> showed all lines could produce cultures containing >90% hPSC cardiomyocytes, based on staining for alpha-actinin (Figure S4A).

Using this differentiation strategy, we also sought to evaluate expression levels of a selected gene set to establish the time point at which future studies were conducted. Over a 66-day time course of differentiation, quantitative real-time PCR showed expression level stabilized by day 30–40 for *ADRB1*, *ADRB2*, *GRK2*, *GRK5*, and *ARRB2* (Figure S4B). Interestingly, the profile of *ARRB1* appeared to differ between the  $\beta_2$ AR variant lines, but these levels also stabilized after day 30. Thus, all further experiments were conducted using hPSC-cardiomyocytes of day 30–40 differentiation.

Signaling via the  $\beta_2$ AR functions through adenylate cyclase to produce the second messenger, cAMP.<sup>26</sup> Therefore, to assess whether cardiomyocytes from isogenic lines carrying polymorphic receptor isoforms possessed  $\beta_2$ AR-specific pharmacology, we used a radioactive cAMP accumulation assay. In this assay, the addition of 3-isobutyl-1-methylxanthine (IBMX), a phosphodiesterase inhibitor, inhibits the typical and rapid intracellular breakdown of cAMP. To allow detection of weaker responses (e.g.,  $\beta_1$ AR) we extended incubation time to 5 h.

In all four lines, isoprenaline, a non-selective  $\beta_2$ AR competitive agonist, produced a concentration-dependent increase in 3H-cAMP accumulation (Figure 2). In the presence of 100 nM of ICI 118551, a selective  $\beta_2$ AR antagonist, a rightward shift in the concentration response curve was observed. However, no shift was detected when CGP 20712A, a selective  $\beta_1$ AR antagonist, was used. The low



**B**

**GE** TTGCTGGCACCCAATGGAAGCCATGCGCCGGACCACGACGTCACGCAGGAAAGGGACGAG  
**GQ** TTGCTGGCACCCAATGGAAGCCATGCGCCGGACCACGACGTCACGCAGCAAAGGGACGAG  
**RE** TTGCTGGCACCCAATAGAAGCCATGCGCCGGACCACGACGTCACGCAGGAAAGGGACGAG  
**RQ** TTGCTGGCACCCAATAGAAGCCATGCGCCGGACCACGACGTCACGCAGCAAAGGGACGAG  
 \*\*\*\*\*

**GE** GTGTGGGTGGTGGGCATGGGCATCGTCATGTCTCTCATCGTCCTGGCCATCGT  
**GQ** GTGTGGGTGGTGGGCATGGGCATCGTCATGTCTTTAATCGTCCTGGCCATCGT  
**RE** GTGTGGGTGGTGGGCATGGGCATCGTCATGTCTTTAATCGTCCTGGCCATCGT  
**RQ** GTGTGGGTGGTGGGCATGGGCATCGTCATGTCTTTAATCGTCCTGGCCATCGT  
 \*\*\*\*\*

**Figure 1. Generation of CRISPR-Cas9/PiggyBac-mediated isogenic models for ADRB2 polymorphisms**

(A) Targeting strategy, demonstrating (1) relative polymorphic positions rs1042713 and rs1042714 are represented by homozygous GGA and GAA within HUES7 ADRB2 gene locus. The thin line corresponds to genomic area surrounding ADRB2 gene, and black boxes indicate main ORF as well as uORF situated within 5'UTR. 5' and 3'UTRs are also shown (medium size black box); position of targeting cassette integration/excision point is indicated by dashed red line. (2) Donor targeting vector: thin circular line corresponds to background targeting plasmid, PuroΔTK selection cassette flanked by 5'/3' PiggyBac terminal repeat (TR) regions (ITR, arrow type boxes) as indicated. PGK promoter and bGH polyadenylation site (pA) are also highlighted; regions of 1 kb of each left and right ADRB2 flanks are bordered by dashed lines. (3) ADRB2 recombined locus: intermediate step after integration of selection cassette into desired position by homologous recombination. (4) ADRB2 final isogenic lines: modified ADRB2 locus, restored after excision of resistance cassette by PiggyBac transposase and carrying modified ADRB2 gene with introduced polymorphic variants. (5) Red arrows indicate positions of primers used for genotyping. (B) Aligned sequences surrounding sites of genome-editing manipulations including positions 46 and 79 and positions 124 and 126 (note resulting TTAA sequence). Original sequencing results confirming correct editing are shown in Figure S1.

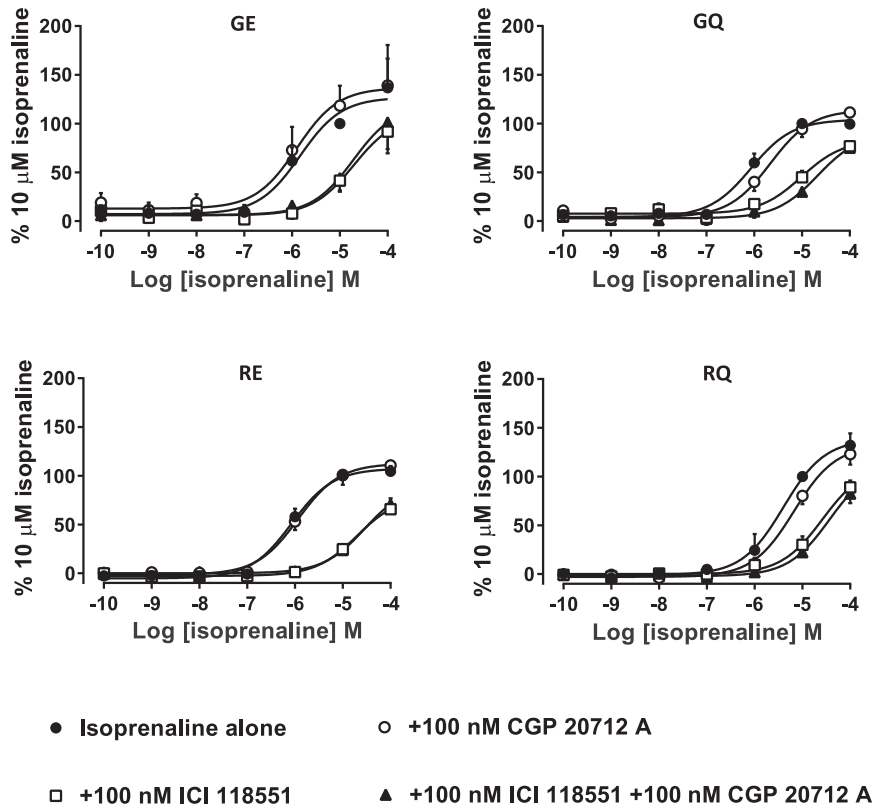


**Figure 2.  $\beta_2$ AR-specific pharmacology preserved in cardiomyocytes derived from isogenic  $\beta_2$ AR polymorphism-specific cell lines**

$^3$ H-cyclic AMP accumulation in response to isoprenaline and in the presence or absence of subtype-specific antagonists ( $\beta_1$ AR-CGP 20172A,  $\beta_2$ AR-ICI 118551). Cardiomyocytes show very specific  $\beta_2$ AR pharmacology, with nearly absent  $\beta_1$ AR response. Data points are presented as means  $\pm$  SEM. Experiments were performed in triplicate ( $n = 5$ – $7$  measurements per condition, depending on treatment).

tive increases in concentration of isoprenaline (0.1–100 nM) were used as an agonist, allowing  $\beta_2$ AR responses to be isolated by preincubating with the  $\beta_1$ AR blocker (CGP 20712A, 100 nM). GE showed the highest sensitivity to  $\beta_2$ AR stimulation, with an  $EC_{50}$  of 1 nM, similar to RE, yet significantly different (4 nM; Figure 3). Substitution of E27 to Q27 (i.e., GE to GQ and RE to RQ) showed much more dramatic reduction in sensitivity compared to both GE and RE variants, with an  $EC_{50}$  of 31 nM (GQ) and 29 nM (RQ). These data suggest that  $\beta_2$ AR polymorphism in position 27 (E to Q) has a strong effect on immediate cAMP response to ligand stimulation in hPSC-cardiomyocytes, whereas position 16 (G to R) plays a more minor role. However, stimulation with isoprenaline might differentially affect immediate changes in expression of variant-specific  $\beta_2$ ARs, which in turn could impact the kinetics of cAMP production.

#### Differential hPSC-cardiomyocyte contractility in $\beta_2$ AR variants in normal and stressed conditions

We then decided to evaluate whether differences observed between hPSC-cardiomyocytes from  $\beta_2$ AR variant-specific lines in immediate cAMP response associated with altered contractile behavior under normal and stressed conditions. Monitoring beating rate following  $\beta_2$ AR stimulation with isoprenaline in the presence of the  $\beta_1$ AR blocker CGP 20712A (300 nM) showed GE rate increased by 2.3-fold within the first 2 min. This rate reduced by 5 min and stabilized at 1.7-fold higher than that of basal contractility by 20 min post-treatment (Figure 4, Control). In comparison, GQ cardiomyocytes had a contractility rate of 1.8-fold greater than basal rate when treated with isoprenaline, which steadily decreased over the 20-min isoprenaline stimulation before returning to basal levels. The RQ cell line showed the least increase in contractility after isoprenaline treatment, a 1.4-fold increase from that of basal. Surprisingly, RE cardiomyocytes showed no significant change in contractility from baseline upon isoprenaline stimulation.

To assess the effect of  $\beta_2$ AR stimulation on beating rate during cardiac stress, hPSC-cardiomyocytes were subjected to a simulated adrenaline shock model.<sup>31</sup> Thus, all 4 lines were challenged by

half-maximal effective concentration ( $EC_{50}$ ) observed here (as compared to data shown in Figure 3) is most likely due to the time-scale of the experiment. During the 5-h cAMP measurements, the  $\beta_2$ AR will have undergone significant desensitization, hence shifting the  $EC_{50}$  values to higher agonist concentrations and bringing them close to the agonist equilibrium dissociation constant ( $K_D$ ) values.<sup>27</sup> These data indicated that  $\beta_2$ AR-mediated pharmacological responses predominate over  $\beta_1$ AR in cardiomyocytes from these isoform-specific hPSC lines. Although we detected expression of both *ADRB1* and *ADRB2* mRNAs, only  $\beta_2$ AR presents detectable activity and therefore is the dominant receptor type. Our data on dominance of  $\beta_2$ AR over  $\beta_1$ AR activity in hPSC-cardiomyocytes is in concordance with previous findings.<sup>28</sup>

Collectively, we created an isogenic set of *ADRB2* gene edited variants that retain characteristics of hPSCs. This includes high-efficiency differentiation into cardiomyocytes, in which gene expression stabilized by day 30–40 to give a specific  $\beta_2$ AR cAMP accumulation pharmacological profile.

#### Sensitivity of hPSC-cardiomyocytes to isoprenaline is dependent on $\beta_2$ AR polymorphisms

To determine whether specific polymorphic combinations influence immediate cAMP production in hPSC-cardiomyocytes, we used real-time fluorescence resonance energy transfer (FRET) microscopy to calculate the  $EC_{50}$  in response to  $\beta_2$ AR stimulation.<sup>29,30</sup> Cumula-

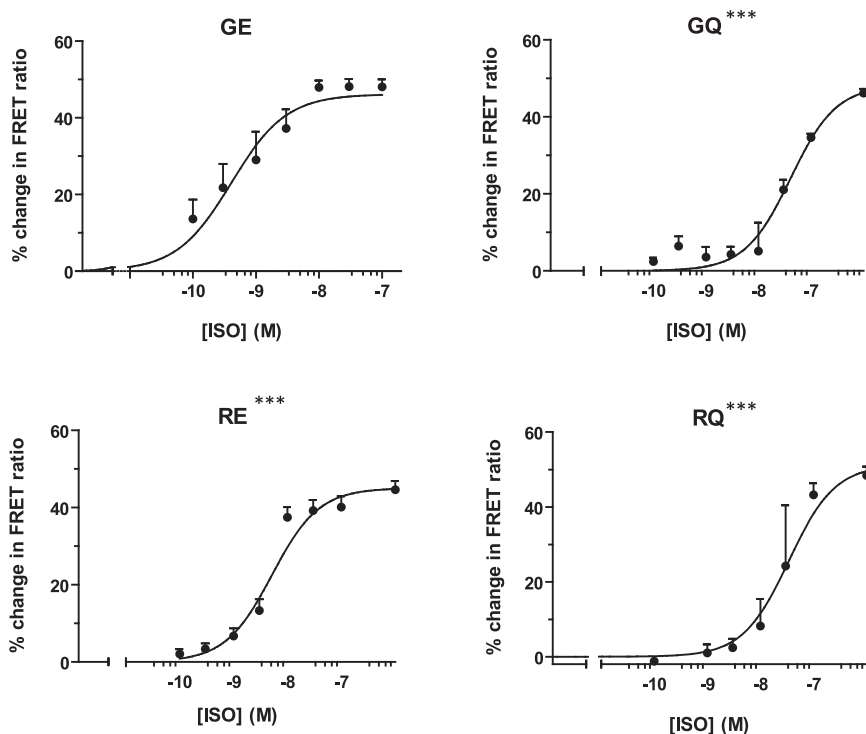


**Figure 3. Concentration-response curves to increasing concentrations of isoproterenol (ISO)**

The  $EC_{50}$  of the 4  $\beta_2$ AR isoforms in hiPSC-CM were calculated in response to  $\beta_2$ AR stimulation with isoprenaline in the presence of 100 nM CGP20172A and measured using real-time FRET microscopy. Upon obtaining a stable baseline after  $\beta_1$ AR inhibition,  $\beta_2$ ARs were stimulated by stepwise increments of isoprenaline concentration. The response was recorded until a plateau was reached for each increment, typically a maximum of 10 min, before the addition of the next isoprenaline solution. Overall time of experiment, including baseline recording, was 60 min. cAMP response normalized to NKH. FRET values are presented as means  $\pm$  SEM. N values are as follows (n/N, where n = experiments and N = batch preparations): GE (4/2), RQ (3/2), RE (9/4), and GQ (4/4). Significantly different from GE, \*\*\*p < 0.001, F-test.

#### Downregulation of cAMP response is polymorphism dependent in hPSC-cardiomyocytes

Prolonged stimulation of  $\beta_2$ AR with agonists leads to receptor downregulation.<sup>33</sup> To understand whether polymorphic combinations affect the extent of receptor downregulation, we used real-time monitoring of cAMP

pre-treatment with 1  $\mu$ M adrenaline to initiate  $\beta$ AR desensitization or Gi-switching, and then cells were exposed to  $\beta_2$ AR stimulation with isoprenaline in the presence of  $\beta_1$ AR blocker CGP 20712A. Cardiomyocytes expressing the  $\beta_2$ AR GE variant increased beat rate to 1.2-fold basal at 2 min, which remained raised throughout the 20-min isoprenaline treatment. Contractility of GQ cells increased to 0.2-fold at 2 min but returned to basal levels after 20 min of isoprenaline treatment. Interestingly, adrenaline pre-treatment led to the change in cellular contractility of RQ as well as RE cells being completely suppressed (Figure 4A).

To reveal the differences in tonic effect of Gi-switching in depressing beating rate, we treated hPSC-cardiomyocytes with pertussis toxin (PTX), an agent that abolishes the negative chronotropic response of muscarinic or adenosine agonists.<sup>32</sup> While no significant Gi effect was seen for GE, GQ, and RE, we found a significant increase in beating rate in the RQ variant in PTX-treated cells compared to control ( $t[10] = 3.583$ ,  $p = 0.005$ ) over the 20 min of  $\beta_2$ AR stimulation with isoprenaline (Figure 4B).

These results showed that GE variant of  $\beta_2$ AR mediated the strongest effect on cardiomyocyte contractility upon stimulation with isoprenaline. While all combinations of polymorphisms demonstrated differing degrees of desensitization under stress conditions, only the RQ combination responded positively to PTX treatment. Therefore, differential contractility responses observed in  $\beta_2$ AR variant-specific lines could only partially be explained by differences in cAMP response (Figure 3) or coupling to Gi (Figure 4B)

production as a measure of  $\beta_2$ AR activity. Cardiomyocytes from all variant-specific hPSC lines were transfected with Luc-RII $\beta$ -Luc split-luciferase vector<sup>34</sup> and exposed to a saturating concentration of isoprenaline (10  $\mu$ M) for 24 h in order to promote receptor downregulation. Real-time measurement after wash and re-challenge with 1  $\mu$ M isoprenaline showed significant downregulation of  $\beta_2$ AR-mediated cAMP production in all lines when compared to control (Figure 5A; Figure S5A). There was a significant difference in percent cAMP induction for GE relative to GQ (Figure 5B). In addition, there was a trend, albeit non-significant, toward an increased level of downregulation in the GQ isoform relative to RE or RQ. This implies that Gly at position 16 coupled with Gln at position 27 shows the strongest downregulation of  $\beta_2$ AR activity, compared to other polymorphic combinations (Figure 5).

#### Desensitization of cAMP synthesis is dependent on polymorphic combinations

Previous reports using human lymphocytes homozygous for each haplotype group of  $\beta_2$ AR have shown differential effect of polymorphisms on receptor desensitization.<sup>35</sup> To determine whether this held true in the isogenic hPSC-cardiomyocyte model, we again relied on the same split-luciferase-based real-time system to measure cAMP response (see schematic in Figure S6). Cardiomyocytes were treated with 1  $\mu$ M isoprenaline in the presence of CGP 20712A for a period of 30 min or 2 h to induce receptor desensitization. Subsequently, cells were washed, challenged a second time with isoprenaline, and then cAMP production monitored by measurement of luciferase activity. Percentage cAMP was calculated by normalizing to the peak induced

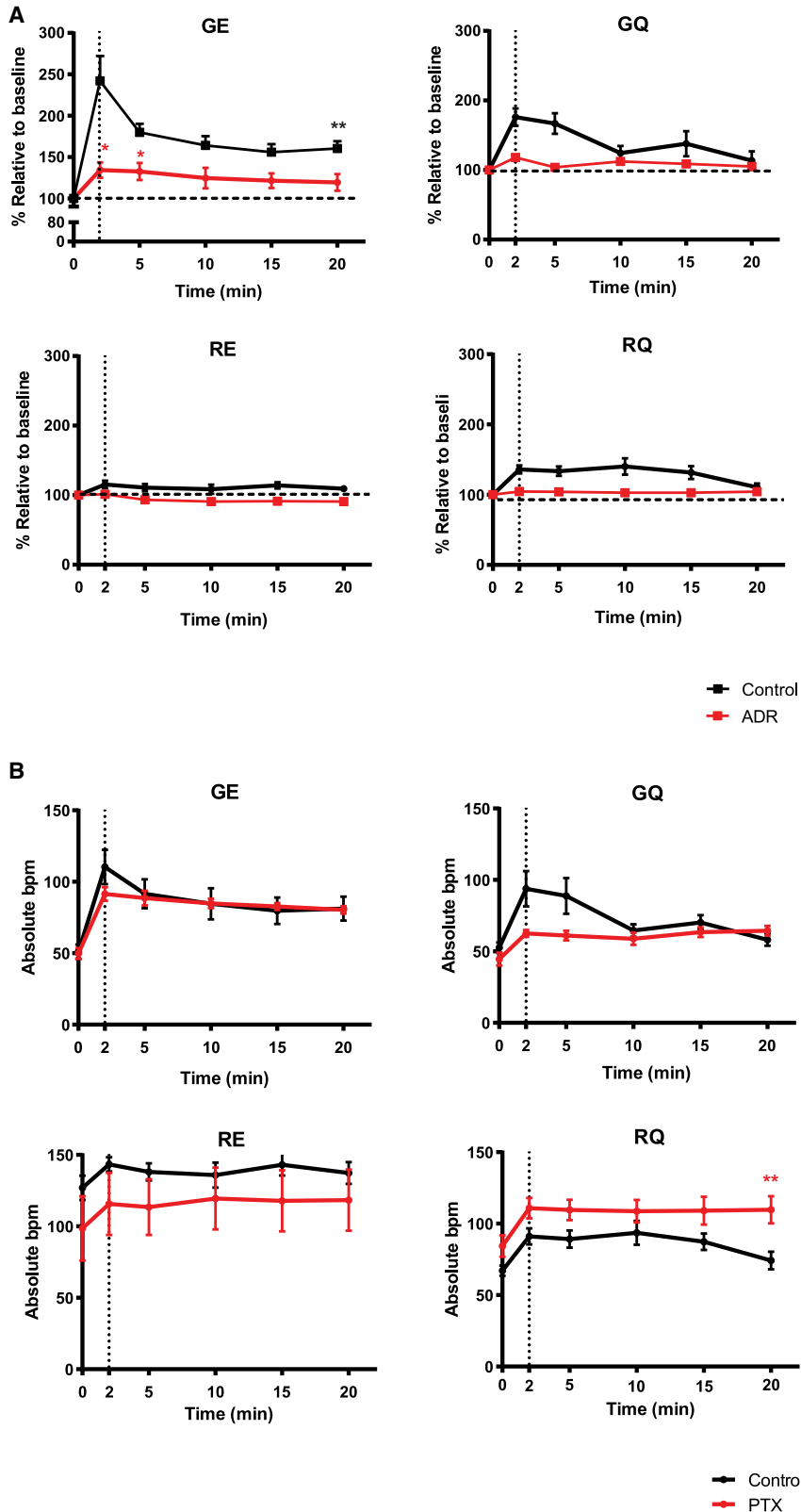


**Figure 4. Contractility response to isoprenaline in unstimulated or stressed  $\beta_2$ AR variant-specific cardiomyocytes**

(A) Increase in beating rate over basal with 0.01  $\mu$ M isoprenaline in the presence of 300 nM CGP20172A. Data presented as mean  $\pm$  SEM. N values (n/N, where n = experiments and N = batch preparations): GE (6/6), GQ (5/5), RQ (6/6), and RE (7/7). Repeated-measures ANOVA. Only GE above basal at 20 min, \*\*p < 0.01;  $\beta_2$ AR response after 20 min pre-treatment with high adrenaline (ADR, red line). (B) Increase in beating rate from baseline with isoprenaline in the presence of  $\beta_1$ AR-blocker CGP20172A in control and PTX-treated cells for each isogenic line. Data shown as absolute beats per minute (bpm) and presented as mean  $\pm$  SEM. N values (n/N, where n = experiments and N = batch preparations) for PTX GE (7/6), GQ (5/5), RQ (6/6), and RE (7/7). Significantly different from control, \*\*p < 0.01.

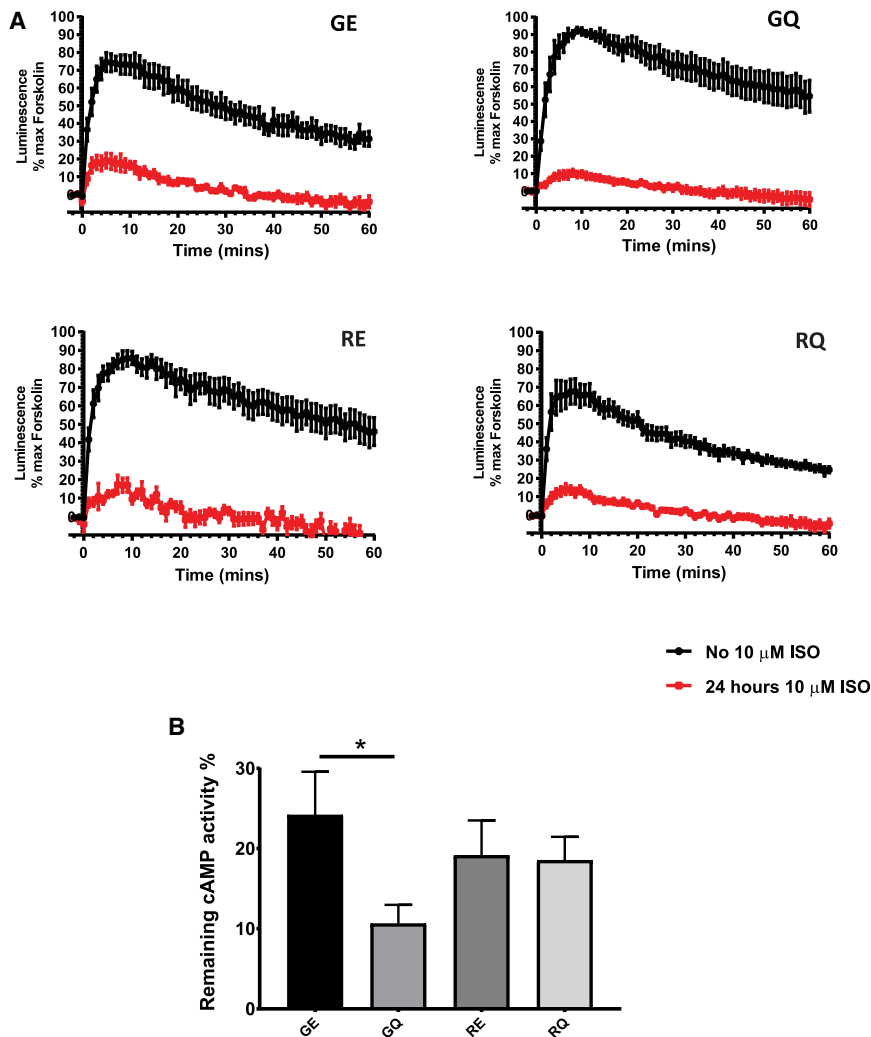


**Figure 5. Downregulation of  $\beta_2$ AR cAMP production in response to prolonged exposure to isoprenaline**

Cardiomyocytes from GE, GQ, RE, and RQ lines were transfected with pGloSensor 20F plasmid and after 48 h were incubated with 10  $\mu$ M isoprenaline for 24 h. After washing, cells were re-challenge with 1  $\mu$ M of isoprenaline and real-time cAMP response was measured. (A) Time course analysis during 1 h after re-challenge. (B) Maximum remaining cAMP response after 24 h exposure to 10  $\mu$ M isoprenaline normalized to maximum untreated control (0 h). cAMP across multiple experiments. Data are presented as means  $\pm$  SEM ( $n \geq 7$ , two-tailed unpaired *t* test; \* $p = 0.0349$ ).

observation that GQ has higher rate of desensitization is in agreement with work using human lymphocytes.<sup>35</sup>

#### Differential toxicity of $\beta_2$ AR variant-specific cardiomyocytes to doxorubicin treatment

The observation that different  $\beta_2$ AR polymorphic isoforms are associated with altered functional responses prompted us to investigate whether this extended to variability in drug-induced cardiotoxicity.<sup>36,37</sup> While it is known that  $\beta_2$ AR is associated with sensitivity to doxorubicin,<sup>38,39</sup> the influence of different polymorphic variants of the receptor has not been explored. Since the RE combination is almost absent in the human population, and therefore has no clinical significance, it was omitted from the following experiments. Using release of lactate dehydrogenase (LDH) as a measure of cell death,<sup>37,40</sup> we found that all isogenic hPSC-cardiomyocyte lines showed substantial toxicity after 24 h of exposure to doxorubicin at 3 and

by forskolin treatment, which causes nonspecific activation of adenylate cyclases and release of maximum potential cAMP (Figure 6; Figure S5).

Significant reduction of cAMP formation was seen at 30-min and 2-h time points for all  $\beta_2$ AR polymorphic combinations compared to controls, but the magnitude of effect differed (Figure S5B). As before, calculation of the percentage cAMP induction showed a significant reduction in GQ relative to the other three haplotypes at the 2-h time point, consistent with the high sensitivity of this variant (Figure 6B; Figure S5B). Interestingly, GE also showed a tendency toward reduced percentage of cAMP induction relative to RE and RQ. Pre-treatment of hPSC-cardiomyocytes with CGP 20712A and ICI 118551 before addition of isoprenaline did not cause marked decreases in rate or cAMP production, though it should be noted that the concentrations of the blockers were well below those to induce inverse agonism.

These data suggest that  $\beta_2$ AR variants carrying Gly16 show a faster desensitization dynamic compared to Arg16 (Figure 6B), and the

30  $\mu$ M (Figure 7). However, the level of toxicity differed significantly, with GE and RQ showing highest and lowest sensitivity, respectively, and GQ falling between these two extremes. This observation is broadly consistent with other assays we have performed, particularly relating to the GE and RQ cardiomyocytes showing opposing responses, and implies  $\beta_2$ AR isoforms warrant further investigation as predictive genetic markers of toxic response to drugs such as doxorubicin.

#### DISCUSSION

In an attempt to control the limitations of non-physiological expression and variable background genotype, we used CRISPR/Cas9 gene editing approaches to create an isogenic suite of  $\beta_2$ AR polymorphisms in the N terminus of the protein within hPSCs. This afforded the opportunity to produce a renewable resource of functional hPSC-cardiomyocytes for direct inter-comparison, hence determining the impact of the GE, GQ, RQ, and RE homozygous polymorphisms at positions 16 and 27 of the  $\beta_2$ AR. This demonstrated differential responses between the  $\beta_2$ AR variants, particularly regarding sensitivity

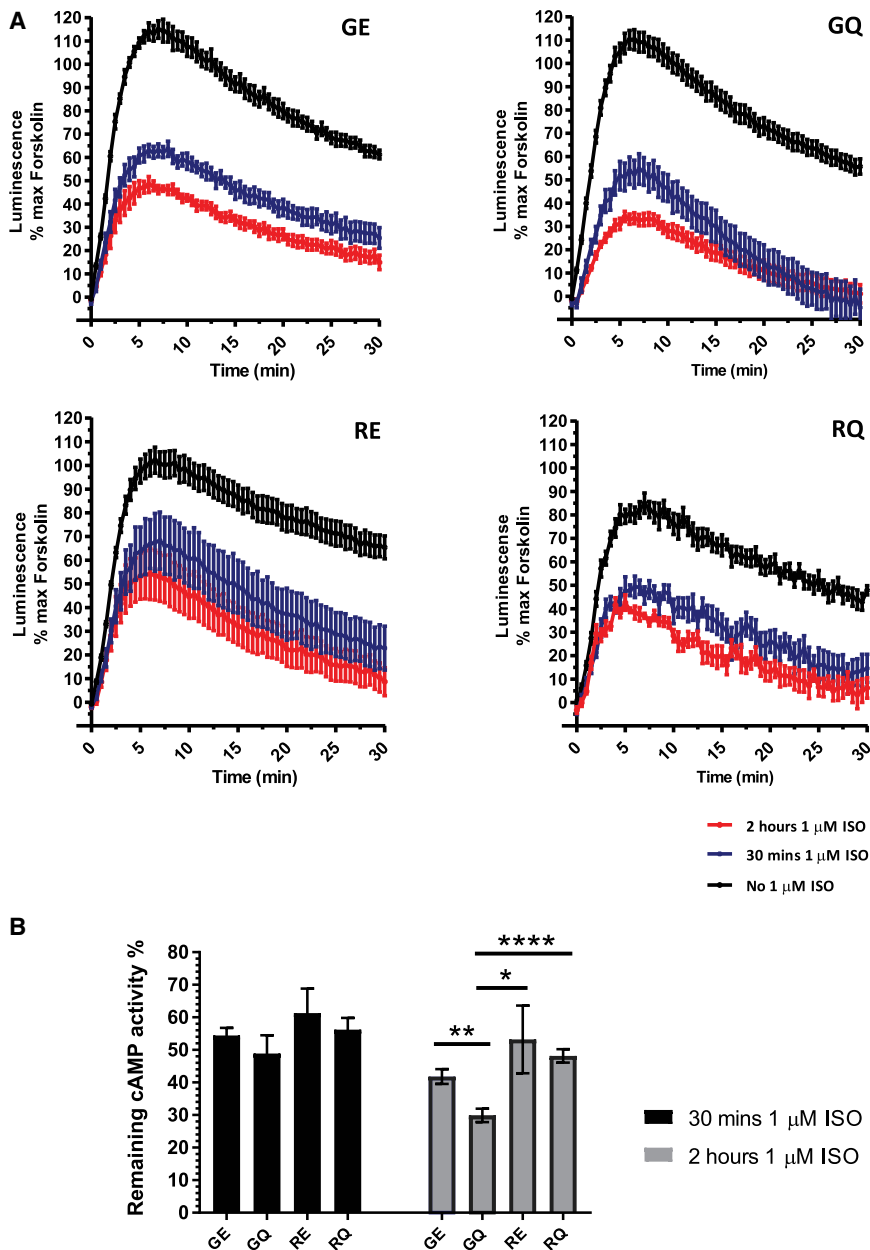


**Figure 6. Isoprenaline-induced desensitization of  $\beta_2$ AR cAMP production**

(A) Time course analysis of the effects of 30 min and 2 h of pre-treatment with 1  $\mu$ M of isoprenaline versus sample treated with vehicle. (B) Comparison of remaining  $\beta_2$ AR-mediated cAMP response to 1  $\mu$ M isoprenaline after pre-treatment with isoprenaline for 0.5 or 2 h. Data are presented as means  $\pm$  SEM ( $n \geq 7$ , two-tailed unpaired  $t$  test, \* $p = 0.0133$ , \*\* $p = 0.0008$ , \*\*\*\* $p < 0.0001$ ).

to modify *ADRB2*, which is a single exon gene with complex 5' and 3' regulatory regions.<sup>42</sup> Nevertheless, we still needed to make subtle adaptations to enable the approach to be employed successfully. Thus, a synonymous change of a leucine codon CTC to TTA was needed to accommodate the requirements of the *PiggyBac* system.<sup>41</sup> We did this to overcome the lack of endogenous TTAA at suitable proximity to the Cas9 cleavage site. In adopting this approach, we considered the potential impact on expression of *ADRB2* but reasoned the main two parameters, codon usage<sup>43</sup> and location in the gene,<sup>44</sup> were relatively risk free. The synonymous change to TTA produces a codon that is already naturally present in *ADRB2*, and it brings its usage frequency close to average observed for human (4.8 versus 7.2<sup>45,46</sup>). Given the fact that *ADRB2* is a low-expression gene, it is unlikely this introduction will place unnecessary demand on the translational machinery<sup>47</sup> and affect expression level of  $\beta_2$ AR. The TTA codon change we made was close to the start of the gene and considered unlikely to modify expression of *ADRB2* due to the effect on stop codon readthrough, since this effect is more commonly associated with changes in the 3' region of the sequence controlling translational termination.<sup>44</sup>

The editing approach also allowed us to examine receptor density between different variants, while not unwittingly changing other parameters. For example, polymorphic variants in the 5' UTR upstream open reading frame (uORF) of the *ADRB2* gene (minus 47 T>C, affecting amino acid at position 19 in the  $\beta_2$  upstream peptide [BUP]), has been found to be in strong linkage disequilibrium with positions 16 and 27 and influence expression of the  $\beta_2$ AR protein.<sup>16,42</sup> Because all the lines we created have the same variant at position minus 47, we can rule this out as a confounding factor in our interpretation of the results.

An unexpected challenge was the low expression levels of  $\beta_2$ AR in hPSC-cardiomyocytes. Our initial attempts to measure receptor density by using radioligand binding assay failed, probably due to low

to isoprenaline, downregulation, desensitization, and doxorubicin-induced cardiotoxicity (DIC). This suggests that further understanding of the  $\beta_2$ AR variants individuals express could be used to guide patient-specific precision medicine approaches.

This study has highlighted the advantages and disadvantages of hPSC-cardiomyocytes as a model system.<sup>23</sup> A key benefit of this human-based system is its high genetic tractability, which provides opportunities to create isogenic suites of genetically normal cells that can be differentiated as a renewable resource to the target cell type of interest, while also retaining physiological levels of gene expression. In our case, we used a "scar-free" CRISPR/Cas9 and *PiggyBac* gene editing approach<sup>41</sup>



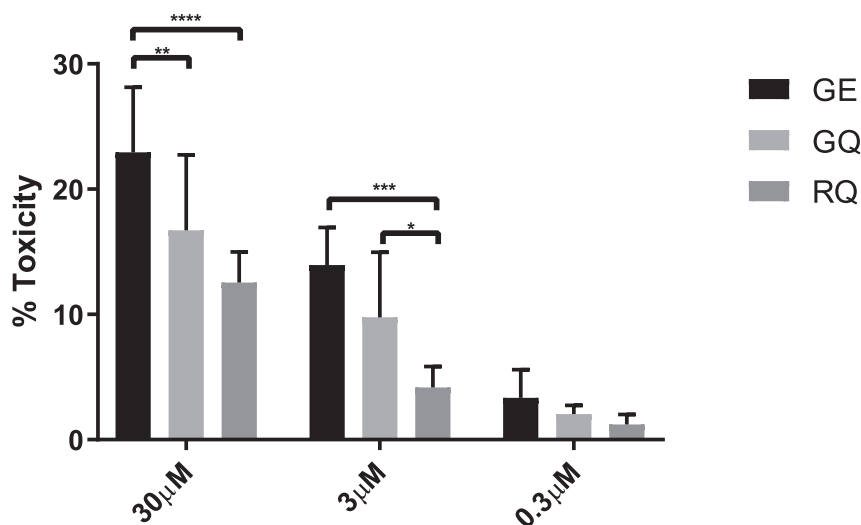


**Figure 7. Doxorubicin-induced toxicity in GE, GQ, and RQ haplotype cardiomyocytes**

Cardiomyocytes from specific lines were treated with 30, 3, and 0.3  $\mu$ M of doxorubicin for 24 h. Toxicity was evaluated by measurement of LDH release. Data are presented as means  $\pm$  SEM ( $n \geq 5$ , \* $p = 0.0199$ , \*\* $p = 0.0027$ , \*\*\* $p = 0.0003$ , \*\*\*\* $p = 0.0001$  two-way ANOVA with Tukey's multiple comparisons test).

level of expressed protein. The signal/noise ratio was not sufficient to provide scope to extract reliable information on specific binding in the presence and absence of our beta-adrenergic antagonists (Figure S7). Our own work (unpublished) and that of others demonstrates that existing  $\beta_2$ AR antibodies lack both sensitivity and specificity to be useful in protein detection in cells with native low levels of  $\beta_2$ AR expression.<sup>48,49</sup> Thus, where immunostaining is performed, overexpression approaches are used to raise signal above background levels. We therefore used differences in maximal cAMP response to isoprenaline as an indirect measure of receptor abundance (Figure S8). The lower density of Arg16-containing variants has been reported before;<sup>50–52</sup> in our case, RQ also showed reduced cAMP max response compared to GE or GQ variants, which can be explained by lower receptor density of RQ.

The potential influence of 5'UTR polymorphisms on receptor density<sup>42</sup> in our model can be excluded since all variants were expressed under the same 5'UTR. An alternative explanation<sup>53</sup> could be that some fraction of the  $\beta_2$ AR population is already desensitized under normal conditions due to spontaneous/constitutive activity, a known characteristic of  $\beta_2$ AR.<sup>54,55</sup> It is possible that different polymorphic variants possess differing degrees of spontaneous activity. An important question for the future will be to include  $\beta_2$ AR in heterozygous or heterozygous/homozygous configurations, since most possible combinations exist in the human population. This was beyond the scope of our study, because conducting a study with the numerous variations and power required, while also accounting for potential subtleties of different allelic-specific expression patterns, will make this a considerable undertaking. Indeed, this notion is supported by our observation of subtle differences in responses between homozygous lines, suggesting that only high powering of analysis across several heterozygous lines in parallel would be sufficient to unveil meaningful differences.

Analyzing response to isoprenaline by measuring the level of cAMP production showed several polymorphism-related differences. We

observed reproducible stronger downregulation of agonist-induced cAMP production in GQ-carrying cardiomyocytes after both prolonged and short exposure to isoprenaline. There was a trend to stronger desensitization after isoprenaline exposure of isoforms with Gly16, both 30-min and 2-h time points. At 2 h, the GQ variant was desensitized to a greater extent than all other haplotype variants. The same tendency remained after prolonged 24-h exposure to a supramaximal concentration of isoprenaline when the GQ variant again showed the lowest cAMP response to  $\beta_2$ AR stimulation, which indicated its high downregulation potential. Similar results, in terms of a greater degree of desensitization to GQ-induced cAMP production at 2 h, were shown in the study by Oostendorp et al.<sup>55</sup> The authors, however, could not observe any haplotype-related differences in desensitization at 30 min or 24 h of treatment.

Our hypothesis that  $\beta_2$ AR variants would have an influence on cardiomyocyte survival following doxorubicin exposure is based on previously published data. First, *ADRB2* gene knockout mice become sensitive to exposure to doxorubicin,<sup>38</sup> an effect that can be reproduced *in vitro* using fibroblasts isolated from these animals.<sup>39</sup> Second, human induced pluripotent stem cell (iPSC)-derived cardiomyocytes were used to recapitulate the phenotype from patients with DIC features.<sup>36</sup> RNA sequencing (RNA-seq) data from this work show unequal distribution of *ARDB2* polymorphic isoforms between affected patients and those not affected by DIC, with GE being absent from patients resistant to treatment. Interestingly, the GE variant showed the highest sensitivity to doxorubicin in our LDH-based assay. The strongest cardioprotective effect against doxorubicin treatment was seen on the RQ isoform.

Differential response to doxorubicin in our experiments could be explained by differential coupling of  $\beta_2$ AR variants to Gi. Indeed, our contractility experiments indicate that different  $\beta_2$ AR N-terminal polymorphism variants might affect Gi coupling of the receptor with RQ, which showed a stronger response to PTX treatment than the other polymorphic combinations (Figure 4B). In agreement with this notion, low association of the Gly16 variant of  $\beta_2$ AR with Gi was recently evidenced by Huang et al.<sup>50</sup> The authors used rat cardiomyocytes transduced with adenoviral vectors expressing polymorphic variants of  $\beta_2$ AR receptor, as well as lymphocytes isolated from genotyped patient carriers. They concluded that the Gly16 variant of

the receptor is Gi defective. The latter, however, is arguable, since most studies on coupling of  $\beta_2$ AR with Gi were done on animal models, and positions 16 and 27 are evolutionarily conserved and occupied by Gly and Glu, respectively.

Notwithstanding these benefits, the hPSC-cardiomyocyte system does have limitations. The differentiated cardiomyocytes produced reach only a limited level of maturity, and this has been well documented in the literature.<sup>23,56</sup> In this study, we found that although levels of *ADRB1* and *ADRB2* mRNA were expressed in hPSC-cardiomyocytes and levels stabilized by day 30–40 of differentiation,  $\beta_2$ AR was predominant at the pharmacological level. Others have described similar findings in hPSC-cardiomyocytes,<sup>28</sup> and these differ from what is known for human adult cardiomyocytes.<sup>57</sup> Moreover, the distribution of  $\beta_1$ AR and  $\beta_2$ AR differs with disease state, with  $\beta_2$ AR typically residing in the t-tubules,<sup>3</sup> structures which form poorly in hPSC-cardiomyocytes. Finally, creating polymorphic variants in hPSCs is recognized as one of the more challenging modifications to achieve, particularly when targeting 2 codons simultaneously to create four homozygous lines. This, coupled with clonal expansion, characterization, long differentiation timelines (30–60 days), costs, and complex phenotyping assays, means carrying this study out in more than one hPSC line was not possible. Indeed, to our knowledge at the time of writing, this is the first time such a set of lines has been created.

It is also acknowledged that, while the work we describe in this report uses cardiomyocytes of human genetic origin, all aspects are carried out *in vitro*. This provides the opportunity to carry out complex genetic modifications, and evaluate receptor function and signaling, and resulting phenotypes such as altered sensitivity to anticancer drugs. Nevertheless, the low receptor density in primary cells meant surrogate assays were required (e.g., for cAMP). Our unpublished data show that forced overexpression of *ADRB2* is not necessarily beneficial, because it compromises differentiation, survival into cardiomyocytes, and native ratios of the  $\beta$ AR isoforms (data not shown), although the overexpressed SNAP-tagged SNP variants showed receptor  $\beta_2$ AR localization consistent with previous reports.<sup>20</sup> Future work will be to repeat these experiments using endogenous expression levels. However, this will require careful Cas9/CRISPR engineering of SNAP-tagged SNP variants of  $\beta_2$ ARs to ensure the complex elements in the 5' and 3' UTRs are not disrupted, since these are essential in regulating expression, processing, and membrane targeting.<sup>16,42</sup>

A complementary approach to the hPSC-cardiomyocyte model would be to make the modifications in mice, particularly given that positions 16 and 27 of *Adrb2* are occupied by Gly and Glu, respectively, hence similar to humans. This would allow the impact of the polymorphisms to be investigated *in vivo* using Cas9/CRISPR editing. However, species differences between mice and humans influence cardiac function and physiology,<sup>56</sup> which extend to divergence  $\beta_1$ : $\beta_2$ AR ratio, cAMP production, and Gi/Gs signaling.<sup>58</sup>

A strength of the hPSC-cardiomyocyte system is the potential to investigate polymorphisms that vary in their impact on phenotype

and function from overtly disease-causing through to more subtle modifiers, and we have published data at both ends of the spectrum.<sup>59,60</sup> While polymorphisms that modify phenotype are often common variations rather than mutations or rare polymorphisms and hence are often undetected in minor allele frequency (MAF)-related searches,<sup>61</sup> they are important. Examples are D/I variant in ACE, associated with the COVID-19 pandemic,<sup>62</sup> or Q41L in GRK5<sup>63</sup> and G16R/E27Q in  $\beta_2$ AR, associated with altered signaling in the heart.<sup>50</sup> Given that  $\beta$ -blockers are one of the most prescribed medicines worldwide<sup>64,65</sup> and the body of literature indicates the importance of the position 16/27 polymorphisms in  $\beta_2$ AR,<sup>1,2,9–15,50,65–67</sup> we elected to study these variants in the context of hPSC-cardiomyocytes.

In conclusion, we developed a human-based model system to allow systematic analysis of mechanisms of regulation of  $\beta_2$ AR-mediated cellular response under conditions of toxic stress. This will allow important subtleties of polymorphisms in  $\beta_2$ AR to be unraveled, including the life cycle of these receptors during stimulation, phosphorylation, and induction of alternative signaling pathways. The value of this is evident, given the double-edged sword nature of the  $\beta_2$ AR. While in the heart the  $\beta_2$ AR offers protection to cardiomyocytes by activating the Gi pathway,<sup>31</sup> in the cancer setting it enhances invasiveness upon stimulation.<sup>68,69</sup> Understanding the effect of  $\beta_2$ AR polymorphisms on cardiac response to anticancer therapy would have immediate clinical impact and will help to choose more accurate therapy prescriptions. Having additional tools to evaluate the balance between these outcomes will be vital to define risk and benefit of drugs such as beta-blockers in precision medicine.

## MATERIALS AND METHODS

### Cell culture and reagents

All culture was at 37°C at 5% CO<sub>2</sub> in a humidified atmosphere. Unless otherwise stated, all reagents were from Thermo Fisher. HUES7 hESCs were gifted by Chad Cowan and Doug Melton at the Harvard Stem Cell Institute. Culture was in E8 medium on Matrigel, although initial culture processes were done in hESC medium conditioned using mouse embryonic fibroblasts. Cell harvesting was done using 0.5 mM EDTA for passaging or with Accutase for freezing or before transfections.

### Construction of targeting and guide RNA (gRNA) expression vectors

*ADRB2* targeting vectors was constructed via Gibson assembly by using Gibson Assembly master mix (E2611S, NEB) as described previously.<sup>22</sup> All primers used to create targeting vectors and gRNA-B5 plasmid are listed in Table S1. The general primers set to amplify left (primers P4 and P5) and right *ADRB2* homology arms (primers P6 and P7) from HUES7 gDNA and *PiggyBac* dual drug selection cassette (Puro- $\Delta$ TK, primers P8 and P9) from pMCS-AAT-PB:PGKpuro- $\Delta$ TK (obtained from Wellcome Trust Sanger Institute plasmid repository, Kosuke Yusa laboratory, <http://www.sanger.ac.uk/science/tools/piggybac-transposase-resources>) are as outlined in Table S1. The reaction mixture was used to transform Top10 competent cells, and correct

colonies were identified by restriction digestion analysis and sequencing. The original targeting vector therefore contained GE variant (pADRB2-PB-TARG-GE, GenBank: MT917127; complete sequence is shown in Figure S9) like that of the parental cell line. pADRB2-PB-TARG-RQ targeting vector was created by using the PCR-splice mutagenesis method as described previously.<sup>70</sup> First, we generated two PCR products by amplifying fragment from pSIN-SNAP-ADRB2 plasmid,<sup>71</sup> which encodes the RQ variant of the  $\beta_2$ AR with primer pairs P10 and P11 and a fragment from the pADRB2-PB-TARG-GE template with P12 and P13 primers. Next, two fragments were fused together by PCR-slice reaction, and the resulting hybrid (resulting from PCR by flanking primers P10 and P13) was digested with NcoI restriction enzyme cloned into NcoI-digested pADRB2-PB-TARG-GE backbone, giving pADRB2-PB-TARG-RQ. GQ and RE variants were initially constructed within pSIN-SNAP-ADRB2 background by PCR-splice mutagenesis using the pairs of overlapping primers: P14 and P15 for RE, and P16 and P17 for GQ. The resulting pSIN-SNAP-ADRB2(RE) and pSIN-SNAP-ADRB2(GQ) were used to create pADRB2-PB-TARG-RE and pADRB2-PB-TARG-GQ in a similar way as for pADRB2-PB-TARG-RQ, as described above. We created two SNP-specific gRNA-vectors (gRNA-B5 to target position 48 and gRNA-A1 to target position 79 on *ADRB2* locus respectively; see Figure S1A). gRNA-A1 was described previously.<sup>22</sup> To generate B5, we followed the recommendation of Addgene for constructing gRNA\_Cloning Vector (Addgene, #41824)-based plasmids with Afl II digestion, following Gibson assembly reaction.<sup>72,73</sup> Primers P18 and P19 were used to prepare an insert for Gibson reaction.

### Targeting of *ADRB2* locus

We described previously our targeting approach for using a combination of *PiggyBac* and CRISPR/Cas9 techniques.<sup>22</sup> In brief, for targeting experiments, HUES7 cells were seeded on Matrigel-coated 6-well plates at density  $3 \times 10^5$  cells per well. Twenty-four hours later, cells were transfected by 3.3  $\mu$ g three CRISPR plasmid components (targeting vector, gRNA vector, and Cas9 expressing plasmid) by using FuGene HD transfection reagent according to manufacturer recommendations (Promega). After selection on puromycin (0.25  $\mu$ g/mL), clones were manually picked up and PCR genotyped before selecting them for the transposase excision step. For cassette excision, selected clones were expanded and seeded on 6-well plates before transfection by transposase expression vector pCMV-hyPBBase (obtained from Wellcome Trust Sanger Institute plasmid repository, Allan Bradley laboratory, <http://www.sanger.ac.uk/science/tools/piggybac-transposase-resources>) as described above. Cells were reseeded to 10 cm plates and maintained in culture for 2 to 3 additional days to allow cassette excision by transposase and then exposed to 2  $\mu$ g/mL of ganciclovir (Invivogene) for negative selection. Second-step selection clones were manually dissected and genotyped using primers shown in Table S1. Some clones had excision only from one allele and showed presence of cassette in remaining alleles, so were not chosen for further experiments. Nevertheless, these “incomplete excisions” confirm correct biallelic insertion of cassette during the first targeting step and absence of potential large

deletions in alternative alleles, which can be the result of Cas9-mediated cleavage.<sup>25</sup> Selected clones were also checked for absence of off-targets (see Figures S10 and S11) before performing experiments. We tested all candidates with potential to disrupt gene coding areas for both gRNA-A1 and gRNA-B5. All primers used are indicated in Table S1, and gene target names are presented in Figures S10 and S11. PCR conditions for off-target detection were as described previously.<sup>22</sup>

### Monolayer cardiac differentiation

The monolayer cardiac differentiation process was conducted as previously described.<sup>22</sup> Briefly, the cell lines were first seeded at 40,000 cells/cm<sup>2</sup> in a Matrigel-coated T25 flask and cultured in E8 medium until reaching 80% confluence. Once the confluence was reached, the culture was pre-conditioned using StemPro34 medium containing 1 ng/mL BMP4 (bone morphogenetic protein 4) and Matrigel (1:100) 1 day before starting the differentiation process. On day 0, the confluent culture was treated with StemPro34 medium supplemented with 10 ng/mL of BMP4 and 8 ng/mL of Activin-A for 48 h. On day 2 post differentiation, the medium was switched into RPMI medium with added B27 (minus insulin) supplement and 10  $\mu$ M of KY02111 and XAV939 (KYX). On day 4, the medium was changed into RPMI supplemented with B27 and 10  $\mu$ M of KYX. After 48 h, the medium was changed into RPMI/RB27 (RB27), and the differentiated cells were maintained in it. The signs of beating started from day 6 to day 8 after initiation of the differentiation process.

### Real-time PCR

Total RNA from cells of days 0, 20, 30, 40, 50, and 60 post cardiac differentiation was extracted using the NucleoSpin RNA purification system (Macherey-Nagel) according to manufacturer recommendation. cDNA was produced from 250 ng of total RNA by SuperScript III Reverse Transcriptase. The qPCR reaction was conducted by TaqMan Fast Advanced Master Mix on the Applied Biosystems 7500 Fast Real-Time PCR instrument. Relative expression of genes was calculated and expressed as  $2^{-\Delta\Delta Ct}$ . Expression values were normalized against expression of *GAPDH* as housekeeping gene. TaqMan assay IDs for *GAPDH*, *ADRB1*, *ADRB2*, *GRK2* (*ADRK1*), and *GRK5* are Hs02786624\_g1, Hs02330048\_s1, Hs00240532\_s1, Hs00176395\_m1, and Hs00992173\_m1, accordingly.

### [<sup>3</sup>H]Cyclic AMP accumulation

The accumulation of tritiated cyclic AMP was assessed as described previously<sup>27</sup> with the following modifications. Cardiomyocytes were plated at a density of 100,000 cells per well in 48-well plates and maintained until aged between 30 and 40 days in growth medium (RPMI 1640 medium-B27 supplement, Thermo Fisher). Cells were pre-labeled with [<sup>3</sup>H]adenine (2  $\mu$ Ci/mL) for 2 h at 37°C in 1 mL/well growth medium. Following [<sup>3</sup>H]adenine removal and washing, either ICI 118551 or CGP 20712A (1 pM–10  $\mu$ M) or 10  $\mu$ M isoprenaline was added in growth medium containing the phosphodiesterase inhibitor IBMX (1 mM) to wells and allowed to incubate for 5 h prior to termination of reaction by the addition of 50  $\mu$ L concentrated HCL.

### cAMP measurements via FRET

System set-up: FRET microscopy system consisted of an ORCA-ER CCD (Hamamatsu Photonics) camera attached to an inverted Nikon TE2000 microscope with a 100 W halogen lamp illuminator and EX436/20 excitation filter. The fluorescent light emitted from the object was split into YFP and CFP channels by Quad view beam splitter equipped with a DM455 dichroic mirror and 535/40 and 480/30 emission filters. Recorded images were analyzed by quantifying the relative ratio of YFP to CFP using Micro-Manager1.4 software package. The FRET ratio responses are presented at normalized data to the maximal cAMP released by activation of AC by NKH-477, a forskolin analog (Sigma-Aldrich). JetPRIME (Ployplus) transfection kit was used to transfect hESC-CM with the FRET-biosensor mTurquoise-Epac1-Venus-Venus (pTEV)<sup>74</sup> utilizing the EPAC1 binding domain following manufacturer's protocol. In brief, 200 ng of plasmid was diluted in 50  $\mu$ L of jetPRIME buffer and vortexed for 10 s. To this, 2  $\mu$ L of jetPRIME reagent was added and vortexed for 15 s before incubating at room temperature for 10 min. The transfection mixture was added to the cells in culture dishes containing 1.5 mL culture medium (RPMI + B27) and incubated for 24–72 h before use. For all FRET experiments, cells were seeded in MatTek dishes with a maximum volume of 2.5 mL. All reagents were prepared using a FRET buffer (NaCl 144 mM, HEPES 10 mM, MgCl<sub>2</sub> 1 mM, KCl 5 mM [pH 7.4]) at the following concentrations: CGP 20712A 100 nM, isoprenaline 100 nM, NKH 10  $\mu$ M.

### IonOptix system for contraction measurements

System set-up: cell contractility was measured using an IonOptix system, which consisted of a Nikon TE-200 inverted microscope and a MyoCam CCD Digital Camera (IonOptix) attached to the computer. Contractility recordings were analyzed using the IonWizard package. The behavior of  $\beta_2$ AR on cellular contractility upon stimulation with a number of pharmacological agents was assessed. All reagents were prepared in Krebs-Henseleit (KH) solution at the following concentrations: CGP 20712A 300 nM, isoprenaline 10 nM, NHK 10  $\mu$ M, adrenaline 1  $\mu$ M, PTX 1.5  $\mu$ g/mL. Cells were perfused with the solutions at 37°C for at a rate of 2 mL/min. Initial KH was to obtain a stable baseline beating rate to which treatment responses have been normalized. Protocols established to assess the contractile response of  $\beta_2$ AR stimulation are as follows: control  $\beta_2$ AR response: 15 min KH, 10 min selective  $\beta_1$  blocker CGP 20712A, followed by 20 min isoprenaline + CGP 20712A. *In vitro* stress model by pre-treating cells with adrenaline: 15 min KH, 20 min adrenaline, then 10 min CGP 20712A, then 20 min isoprenaline + CGP 20712A. To assess the influence of G<sub>i</sub> proteins on cellular contractility: cells were pre-treated with PTX (1.5  $\mu$ g/mL for 3 h at 37°C), before 15 min KH perfusion, 10 min CGP 20712A, and then 20 min isoprenaline + CGP 20712A. To assess the role of G<sub>i</sub> proteins on cellular contractility during induced cardiomyocyte stress: cells were pre-treated with PTX as described above, then perfused with KH, 20 min adrenaline, 10 min CGP 20712A, and then 20 min isoprenaline + CGP 20712A.

### Downregulation assay

The  $\beta_2$ AR isoform-specific (GE, GQ, RE, and RQ) cardiomyocytes, at density 30,000 cells/well, were transiently transfected with pGloSensor 20F (Promega) 0.1  $\mu$ g plasmid DNA per well of a 96-well plate using Lipofectamine 3000. At 24 h after transfection, cells were changed into normal RB27 medium and allowed to maintain for 48 h. 24 h prior to the assay, cells were treated with 10  $\mu$ M isoprenaline to stimulate downregulation. Cells were incubated at 37°C for 2 h in RB27 medium supplemented with 25 mM HEPES, 10% fetal bovine serum (FBS), and 2% GloSensor cAMP Reagent stock solution with  $\beta_1$ AR blocker 200 nM CGP 20712A and with/without isoprenaline 10  $\mu$ M. Each condition was performed in triplicate. Washouts were performed by removing GloSensor cAMP reagent mix/incubation medium, washing twice with fresh wash medium (RB27) without isoprenaline in total duration of 10 min, and then adding replacement GloSensor cAMP mix medium with CGP 20712A but without isoprenaline. Control wells received the same number of washes in the same volume of wash medium without isoprenaline. Luminescence was read on EnVision Plate Reader (PerkinElmer) in a temperature-controlled chamber at 37°C. Basal/baseline signal was measured for 20 min. Isoprenaline was added to wells at 1  $\mu$ M final concentration to re-challenge the system, and luminescence was read for 60 min. Later, 10  $\mu$ M forskolin was added to wells to stimulate total cAMP, and luminescence was read for another 30 min. Signal was measured by normalizing to maximum forskolin and subtracting the baseline. Three separate experiments, each done in triplicate, were quantitated and analyzed using Microsoft Excel and GraphPad Prism.

### Real-time measurement of $\beta_2$ AR desensitization

The  $\beta_2$ AR variant (GE, GQ, RE, and RQ) cardiomyocytes, at density 30,000 cells/well, were transiently transfected with pGloSensor 20F (Promega) 0.1  $\mu$ g plasmid DNA per well of 96-well plates using Lipofectamine 3000. At 24 h after transfection, cells were changed into normal RB27 medium and allowed to grow for 48 h. Cells were incubated at 37°C for 2 h in RB27 medium supplemented with 25 mM HEPES, 10% FBS, and 2% GloSensor cAMP Reagent stock solution with  $\beta_1$ AR blocker 200 nM CGP 20712A. At the start of pre-incubation, final concentration of 1  $\mu$ M isoprenaline was added at 2-h and 30-min time points. Each condition was performed in at least duplicate. Washouts were performed by removing GloSensor cAMP reagent mix/incubation medium, washing twice with fresh wash medium (RB27) without isoprenaline in total duration of 10 min, and then adding replacement GloSensor cAMP mix medium with CGP 20712A but without isoprenaline. Control wells received the same number of washes in the same volume of wash medium without isoprenaline. Luminescence was read on EnVision Plate Reader in a temperature-controlled chamber at 37°C. Basal/baseline signal was measured for 10 min. Isoprenaline was added to wells at 1  $\mu$ M final concentration to “re-challenge” the system, and luminescence was read for 30 min. Later, 10  $\mu$ M forskolin was added to wells to stimulate total cAMP, and luminescence was read for another 15 min. Signal was measured by normalizing to maximum forskolin and subtracting the baseline. Three to five separate experiments, each done in

at least duplicate, were quantitated and analyzed using Microsoft Excel and GraphPad Prism.

### Cytotoxicity assays

For doxorubicin toxicity assay, cardiomyocytes were seeded on 96-well plates at 40,000 cells/well. Cells were treated with 30, 3, and 0.3  $\mu\text{M}$  of doxorubicin or vehicle control for 24 h. Cell toxicity was evaluated by using Pierce LDH Cytotoxicity Assay Kit according to manufacturer recommendation.

### Statistical analysis

All statistical analysis was done in GraphPad Prism, version 5.0 or 7.0 (GraphPad Software) as follows: 3H-cyclic AMP accumulations were done as single experiments ( $n = 5-7$ ) and performed in triplicate and mean  $\log\text{EC}_{50}$  values compared using 1-way ANOVA with Tukey's multiple comparison test; 2-way ANOVA with Tukey's multiple comparison test was used for LDH release experiment, and two-tailed unpaired t test was used for downregulation and desensitization assays. Statistical significance between the four haplotypes from FRET experiments were tested using the F-statistic; statistical significance between the four haplotypes from IonOptix contractility experiments were tested using repeated-measure ANOVA.

### SUPPLEMENTAL INFORMATION

Supplemental Information can be found online at <https://doi.org/10.1016/j.omtm.2020.10.019>.

### ACKNOWLEDGMENTS

The authors are supported by the British Heart Foundation (grant numbers SP/15/9/31605, RG/15/6/31436, PG/14/59/31000, RG/14/1/30588, P47352/CRM, and RM/17/1/33377) and the National Centre for the Replacement, Refinement and Reduction of Animals in Research (grant numbers CRACK-IT:35911-259146 and NC/K000225/1). The authors would like to thank Guerout Yorick and Maria Barbadillo-Munoz for technical assistance.

### AUTHOR CONTRIBUTIONS

S.J.H., S.E.H., and C.D. conceived the project; A.K., N.A.N.M.Y., A.H., J.G., T.K., D.H.M., N.T.N.V., and N.D. performed experiments and data analysis; T.M. assisted with some experiments; J.G. provided resources; A.K. and C.D. wrote the paper with editorial input from S.J.H., S.E.H., and J.G.

### DECLARATION OF INTERESTS

The authors declare no competing interests.

### REFERENCES

- Taylor, D.R., and Kennedy, M.A. (2002). Beta-adrenergic receptor polymorphisms and drug responses in asthma. *Pharmacogenomics* 3, 173–184.
- Leineweber, K., and Heusch, G. (2009).  $\beta$  1- and  $\beta$  2-adrenoceptor polymorphisms and cardiovascular diseases. *Br. J. Pharmacol.* 158, 61–69.
- Nikolaev, V.O., Moshkov, A., Lyon, A.R., Miragoli, M., Novak, P., Paur, H., Lohse, M.J., Korchev, Y.E., Harding, S.E., and Gorelik, J. (2010). Beta2-adrenergic receptor redistribution in heart failure changes cAMP compartmentation. *Science* 327, 1653–1657.
- Xiang, Y.K. (2011). Compartmentalization of beta-adrenergic signals in cardiomyocytes. *Circ. Res.* 109, 231–244.
- Communal, C., Singh, K., Sawyer, D.B., and Colucci, W.S. (1999). Opposing effects of beta(1)- and beta(2)-adrenergic receptors on cardiac myocyte apoptosis: role of a pertussis toxin-sensitive G protein. *Circulation* 100, 2210–2212.
- Chesley, A., Lundberg, M.S., Asai, T., Xiao, R.-P., Ohtani, S., Lakatta, E.G., and Crow, M.T. (2000). The  $\beta$ (2)-adrenergic receptor delivers an antiapoptotic signal to cardiac myocytes through G(i)-dependent coupling to phosphatidylinositol 3'-kinase. *Circ. Res.* 87, 1172–1179.
- Woo, A.Y.H., and Xiao, R.P. (2012).  $\beta$ -Adrenergic receptor subtype signaling in heart: from bench to bedside. *Acta Pharmacol. Sin.* 33, 335–341.
- Bernstein, D., Fajardo, G., and Zhao, M. (2011). THE ROLE OF  $\beta$ -ADRENERGIC RECEPTORS IN HEART FAILURE: DIFFERENTIAL REGULATION OF CARDIOTOXICITY AND CARDIOPROTECTION. *Prog. Pediatr. Cardiol.* 31, 35–38.
- Liggett, S.B. (2000). beta(2)-adrenergic receptor pharmacogenetics. *Am. J. Respir. Crit. Care Med.* 161, S197–S201.
- Kay, L.J., Rostami-Hodjegan, A., Suvarna, S.K., and Peachell, P.T. (2007). Influence of beta2-adrenoceptor gene polymorphisms on beta2-adrenoceptor-mediated responses in human lung mast cells. *Br. J. Pharmacol.* 152, 323–331.
- Munakata, M., Harada, Y., Ishida, T., Saito, J., Nagabukuro, A., Matsushita, H., Koga, N., Ohsaki, M., Imagawa, K., and Shiratsuchi, T. (2006). Molecular-based haplotype analysis of the beta 2-adrenergic receptor gene (ADRB2) in Japanese asthmatic and non-asthmatic subjects. *Allergol. Int.* 55, 191–198.
- Sotoodehnia, N., Siscovick, D.S., Vatta, M., Psaty, B.M., Tracy, R.P., Towbin, J.A., Lemaitre, R.N., Rea, T.D., Durda, J.P., Chang, J.M., et al. (2006). Beta2-adrenergic receptor genetic variants and risk of sudden cardiac death. *Circulation* 113, 1842–1848.
- Nakada, T.-A., Russell, J.A., Boyd, J.H., Aguirre-Hernandez, R., Thain, K.R., Thair, S.A., Nakada, E., McConechy, M., and Walley, K.R. (2010). beta2-Adrenergic receptor gene polymorphism is associated with mortality in septic shock. *Am. J. Respir. Crit. Care Med.* 181, 143–149.
- Connor, A., Baumgartner, R.N., Kerber, R.A., O'Brien, E., Rai, S.N., Wolff, R.K., Slattery, M.L., Giuliano, A.R., Risendal, B.C., Byers, T.E., and Baumgartner, K.B. (2012). ADRB2 G-G haplotype associated with breast cancer risk among Hispanic and non-Hispanic white women: interaction with type 2 diabetes and obesity. *Cancer Causes Control* 23, 1653–1663.
- Evans, W.E., and McLeod, H.L. (2003). Pharmacogenomics—drug disposition, drug targets, and side effects. *N. Engl. J. Med.* 348, 538–549.
- Panebra, A., Wang, W.C., Malone, M.M., Pitter, D.R.G., Weiss, S.T., Hawkins, G.A., and Liggett, S.B. (2010). Common ADRB2 haplotypes derived from 26 polymorphic sites direct beta2-adrenergic receptor expression and regulation phenotypes. *PLoS ONE* 5, e11819.
- Bruck, H., Leineweber, K., Beilfuss, A., Weber, M., Heusch, G., Philipp, T., and Brodde, O.E. (2003). Genotype-dependent time course of lymphocyte beta 2-adrenergic receptor down-regulation. *Clin. Pharmacol. Ther.* 74, 255–263.
- Moore, P.E., Laporte, J.D., Abraham, J.H., Schwartzman, I.N., Yandava, C.N., Silverman, E.S., Drazen, J.M., Wand, M.P., Panettieri, R.A., Jr., and Shore, S.A. (2000). Polymorphism of the beta(2)-adrenergic receptor gene and desensitization in human airway smooth muscle. *Am. J. Respir. Crit. Care Med.* 162, 2117–2124.
- Green, S.A., Turki, J., Innis, M., and Liggett, S.B. (1994). Amino-terminal polymorphisms of the human beta 2-adrenergic receptor impart distinct agonist-promoted regulatory properties. *Biochemistry* 33, 9414–9419.
- Koryakina, Y., Jones, S.M., Cornett, L.E., Seely, K., Brents, L., Prather, P.L., Kofman, A., and Kurten, R.C. (2012). Effects of the  $\beta$ -agonist, isoprenaline, on the down-regulation, functional responsiveness and trafficking of  $\beta$ 2-adrenergic receptors with N-terminal polymorphisms. *Cell Biol. Int.* 36, 1171–1183.
- Gough, N.R. (2011). Focus issue: Cracking the G protein-coupled receptor code. *Sci. Signal.* 4, eg7.
- Kondrashov, A., Duc Hoang, M., Smith, J.G.W., Bhagwan, J.R., Duncan, G., Mosqueira, D., Munoz, M.B., Vo, N.T.N., and Denning, C. (2018). Simplified Footprint-Free Cas9/CRISPR Editing of Cardiac-Associated Genes in Human Pluripotent Stem Cells. *Stem Cells Dev.* 27, 391–404.

23. Sala, L., Bellin, M., and Mummery, C.L. (2017). Integrating cardiomyocytes from human pluripotent stem cells in safety pharmacology: has the time come? *Br. J. Pharmacol.* *174*, 3749–3765.
24. Cowan, C.A., Klimanskaya, I., McMahon, J., Atienza, J., Witmyer, J., Zucker, J.P., Wang, S., Morton, C.C., McMahon, A.P., Powers, D., and Melton, D.A. (2004). Derivation of embryonic stem-cell lines from human blastocysts. *N. Engl. J. Med.* *350*, 1353–1356.
25. Kosicki, M., Tomberg, K., and Bradley, A. (2018). Repair of double-strand breaks induced by CRISPR-Cas9 leads to large deletions and complex rearrangements. *Nat. Biotechnol.* *36*, 765–771.
26. Masters, S.B., Sullivan, K.A., Miller, R.T., Beiderman, B., Lopez, N.G., Ramachandran, J., and Bourne, H.R. (1988). Carboxyl terminal domain of Gs alpha specifies coupling of receptors to stimulation of adenylyl cyclase. *Science* *241*, 448–451.
27. Baker, J.G., Hall, I.P., and Hill, S.J. (2002). Pharmacological characterization of CGP 12177 at the human beta(2)-adrenoceptor. *Br. J. Pharmacol.* *137*, 400–408.
28. Wu, H., Lee, J., Vincent, L.G., Wang, Q., Gu, M., Lan, F., Churko, J.M., Sallam, K.I., Matsa, E., Sharma, A., et al. (2015). Epigenetic Regulation of Phosphodiesterases 2A and 3A Underlies Compromised  $\beta$ -Adrenergic Signaling in an iPSC Model of Dilated Cardiomyopathy. *Cell Stem Cell* *17*, 89–100.
29. Niino, Y., Hotta, K., and Oka, K. (2009). Simultaneous live cell imaging using dual FRET sensors with a single excitation light. *PLoS ONE* *4*, e6036.
30. Börner, S., Schwede, F., Schlipp, A., Berisha, F., Calebiro, D., Lohse, M.J., and Nikolaev, V.O. (2011). FRET measurements of intracellular cAMP concentrations and cAMP analog permeability in intact cells. *Nat. Protoc.* *6*, 427–438.
31. Paur, H., Wright, P.T., Sikkil, M.B., Tranter, M.H., Mansfield, C., O’Gara, P., Stuckey, D.J., Nikolaev, V.O., Diakonov, I., Pannell, L., et al. (2012). High levels of circulating epinephrine trigger apical cardiodepression in a  $\beta$ 2-adrenergic receptor/Gi-dependent manner: a new model of Takotsubo cardiomyopathy. *Circulation* *126*, 697–706.
32. Brodde, O.E., and Michel, M.C. (1999). Adrenergic and muscarinic receptors in the human heart. *Pharmacol. Rev.* *51*, 651–690.
33. Moore, R.H., Tuffaha, A., Millman, E.E., Dai, W., Hall, H.S., Dickey, B.F., and Knoll, B.J. (1999). Agonist-induced sorting of human beta2-adrenergic receptors to lysosomes during downregulation. *J. Cell Sci.* *112*, 329–338.
34. Fan, F., Binkowski, B.F., Butler, B.L., Stecha, P.F., Lewis, M.K., and Wood, K.V. (2008). Novel genetically encoded biosensors using firefly luciferase. *ACS Chem. Biol.* *3*, 346–351.
35. Oostendorp, J., Postma, D.S., Volders, H., Jongepier, H., Kauffman, H.F., Boezen, H.M., Meyers, D.A., Bleecker, E.R., Nelemans, S.A., Zaagsma, J., and Meurs, H. (2005). Differential desensitization of homozygous haplotypes of the  $\beta$ 2-adrenergic receptor in lymphocytes. *Am. J. Respir. Crit. Care Med.* *172*, 322–328.
36. Burridge, P.W., Li, Y.F., Matsa, E., Wu, H., Ong, S.-G., Sharma, A., Holmström, A., Chang, A.C., Coronado, M.J., Ebert, A.D., et al. (2016). Human induced pluripotent stem cell-derived cardiomyocytes recapitulate the predilection of breast cancer patients to doxorubicin-induced cardiotoxicity. *Nat. Med.* *22*, 547–556.
37. Holmgren, G., Synnergren, J., Bogestål, Y., Améen, C., Åkesson, K., Holmgren, S., Lindahl, A., and Sartipy, P. (2015). Identification of novel biomarkers for doxorubicin-induced toxicity in human cardiomyocytes derived from pluripotent stem cells. *Toxicology* *328*, 102–111.
38. Fajardo, G., Zhao, M., Berry, G., Wong, L.-J., Mochly-Rosen, D., and Bernstein, D. (2011).  $\beta$ 2-adrenergic receptors mediate cardioprotection through crosstalk with mitochondrial cell death pathways. *J. Mol. Cell. Cardiol.* *51*, 781–789.
39. Fajardo, G., Zhao, M., Powers, J., and Bernstein, D. (2006). Differential cardiotoxic/cardioprotective effects of beta-adrenergic receptor subtypes in myocytes and fibroblasts in doxorubicin cardiomyopathy. *J. Mol. Cell. Cardiol.* *40*, 375–383.
40. Moran, J.H., and Schnellmann, R.G. (1996). A rapid beta-NADH-linked fluorescence assay for lactate dehydrogenase in cellular death. *J. Pharmacol. Toxicol. Methods* *36*, 41–44.
41. Yusa, K., Rashid, S.T., Strick-Marchand, H., Varela, I., Liu, P.-Q., Paschon, D.E., Miranda, E., Ordóñez, A., Hannan, N.R.F., Rouhani, F.J., et al. (2011). Targeted gene correction of  $\alpha$ 1-antitrypsin deficiency in induced pluripotent stem cells. *Nature* *478*, 391–394.
42. McGraw, D.W., Forbes, S.L., Kramer, L.A., and Liggett, S.B. (1998). Polymorphisms of the 5' leader cistron of the human beta2-adrenergic receptor regulate receptor expression. *J. Clin. Invest.* *102*, 1927–1932.
43. Hanson, G., and Collier, J. (2018). Codon optimality, bias and usage in translation and mRNA decay. *Nat. Rev. Mol. Cell Biol.* *19*, 20–30.
44. Jungreis, I., Lin, M.F., Spokony, R., Chan, C.S., Negre, N., Victorson, A., White, K.P., and Kellis, M. (2011). Evidence of abundant stop codon readthrough in *Drosophila* and other metazoa. *Genome Res.* *21*, 2096–2113.
45. Sequence Manipulation Suite: Codon Usage. (2020) [http://www.bioinformatics.org/sms2/codon\\_usage.html](http://www.bioinformatics.org/sms2/codon_usage.html).
46. GenScript. GenScript Codon Usage Frequency Table(chart) Tool. <https://www.genscript.com/tools/codon-frequency-table>
47. Frumkin, I., Lajoie, M.J., Gregg, C.J., Hornung, G., Church, G.M., and Pilpel, Y. (2018). Codon usage of highly expressed genes affects proteome-wide translation efficiency. *Proc. Natl. Acad. Sci. USA* *115*, E4940–E4949.
48. Tsvetanova, N.G., and von Zastrow, M. (2014). Spatial encoding of cyclic AMP signaling specificity by GPCR endocytosis. *Nat. Chem. Biol.* *10*, 1061–1065.
49. Koryakina, Y.A., Fowler, T.W., Jones, S.M., Schnackenberg, B.J., Cornett, L.E., and Kurten, R.C. (2008). Characterization of a panel of six beta2-adrenergic receptor antibodies by indirect immunofluorescence microscopy. *Respir. Res.* *9*, 32.
50. Huang, J., Li, C., Song, Y., Fan, X., You, L., Tan, L., Xiao, L., Li, Q., Ruan, G., Hu, S., et al. (2018). ADRB2 polymorphism Arg16Gly modifies the natural outcome of heart failure and dictates therapeutic response to  $\beta$ -blockers in patients with heart failure. *Cell Discov.* *4*, 57.
51. Eisenach, J.H., Schroeder, D.R., Pavey, E.S., Penheiter, A.R., Knutson, J.N., Turner, S.T., and Joyner, M.J. (2014). Interactions between beta-2 adrenoceptor gene variation, cardiovascular control and dietary sodium in healthy young adults. *J. Physiol.* *592*, 5221–5233.
52. Snyder, E.M., Hulsebus, M.L., Turner, S.T., Joyner, M.J., and Johnson, B.D. (2006). Genotype related differences in beta2 adrenergic receptor density and cardiac function. *Med. Sci. Sports Exerc.* *38*, 882–886.
53. Liggett, S.B. (2002). Polymorphisms of the  $\beta$ 2-adrenergic receptor. *N. Engl. J. Med.* *346*, 536–538.
54. Götz, K., and Jakobs, K.H. (1994). Unoccupied beta-adrenoceptor-induced adenylyl cyclase stimulation in turkey erythrocyte membranes. *Eur. J. Pharmacol.* *268*, 151–158.
55. Bond, R.A., Leff, P., Johnson, T.D., Milano, C.A., Rockman, H.A., McMinn, T.R., Apparsundaram, S., Hyek, M.F., Kenakin, T.P., Allen, L.F., et al. (1995). Physiological effects of inverse agonists in transgenic mice with myocardial overexpression of the beta 2-adrenoceptor. *Nature* *374*, 272–276.
56. de Korte, T., Katili, P.A., Mohd Yusof, N.A.N., van Meer, B.J., Saleem, U., Burton, F.L., Smith, G.L., Clements, P., Mummery, C.L., Eschenhagen, T., et al. (2020). Unlocking Personalized Biomedicine and Drug Discovery with Human Induced Pluripotent Stem Cell-Derived Cardiomyocytes: Fit for Purpose or Forever Elusive? *Annu. Rev. Pharmacol. Toxicol.* *60*, 529–551.
57. del Monte, F., Kaumann, A.J., Poole-Wilson, P.A., Wynne, D.G., Pepper, J., and Harding, S.E. (1993). Coexistence of functioning beta 1- and beta 2-adrenoceptors in single myocytes from human ventricle. *Circulation* *88*, 854–863.
58. Brito-Martins, M., Harding, S.E., and Ali, N.N. (2008). beta(1)- and beta(2)-adrenoceptor responses in cardiomyocytes derived from human embryonic stem cells: comparison with failing and non-failing adult human heart. *Br. J. Pharmacol.* *153*, 751–759.
59. Mosqueira, D., Mannhardt, I., Bhagwan, J.R., Lis-Slimak, K., Katili, P., Scott, E., Hassan, M., Prondzynski, M., Harmer, S.C., Tinker, A., et al. (2018). CRISPR/Cas9 editing in human pluripotent stem cell-cardiomyocytes highlights arrhythmias, hypocontractility, and energy depletion as potential therapeutic targets for hypertrophic cardiomyopathy. *Eur. Heart J.* *39*, 3879–3892.
60. Kargaran, P.K., Evans, J.M., Bodbin, S.E., Smith, J.G.W., Nelson, T.J., Denning, C., and Mosqueira, D. (2020). Mitochondrial DNA: Hotspot for Potential Gene Modifiers Regulating Hypertrophic Cardiomyopathy. *J. Clin. Med.* *9*, E2349.
61. <https://gnomad.broadinstitute.org/>.

62. Delanghe, J.R., Speeckaert, M.M., and De Buyzere, M.L. (2020). The host's angiotensin-converting enzyme polymorphism may explain epidemiological findings in COVID-19 infections. *Clin. Chim. Acta* 505, 192–193.
63. Liggett, S.B., Cresci, S., Kelly, R.J., Syed, F.M., Matkovich, S.J., Hahn, H.S., Diwan, A., Martini, J.S., Sparks, L., Parekh, R.R., et al. (2008). A GRK5 polymorphism that inhibits beta-adrenergic receptor signaling is protective in heart failure. *Nat. Med.* 14, 510–517.
64. Bangalore, S., Messerli, F.H., Kostis, J.B., and Pepine, C.J. (2007). Cardiovascular protection using beta-blockers: a critical review of the evidence. *J. Am. Coll. Cardiol.* 50, 563–572.
65. Akbar, S., and Alorainy, M.S. (2014). The current status of beta blockers' use in the management of hypertension. *Saudi Med. J.* 35, 1307–1317.
66. Litonjua, A.A., Gong, L., Duan, Q.L., Shin, J., Moore, M.J., Weiss, S.T., Johnson, J.A., Klein, T.E., and Altman, R.B. (2010). Very important pharmacogene summary ADRB2. *Pharmacogenet. Genomics* 20, 64–69.
67. Ahles, A., and Engelhardt, S. (2014). Polymorphic variants of adrenoceptors: pharmacology, physiology, and role in disease. *Pharmacol. Rev.* 66, 598–637.
68. Chang, A., Le, C.P., Walker, A.K., Creed, S.J., Pon, C.K., Albold, S., Carroll, D., Halls, M.L., Lane, J.R., Riedel, B., et al. (2016).  $\beta$ 2-Adrenoceptors on tumor cells play a critical role in stress-enhanced metastasis in a mouse model of breast cancer. *Brain Behav. Immun.* 57, 106–115.
69. Kilpatrick, L.E., Alcobia, D.C., White, C.W., Peach, C.J., Glenn, J.R., Zimmerman, K., Kondrashov, A., Pflieger, K.D.G., Ohana, R.F., Robers, M.B., et al. (2019). Complex Formation between VEGFR2 and the  $\beta_2$ -Adrenoceptor. *Cell Chem. Biol.* 26, 830–841.e9.
70. Kondrashov, A., Meijer, H.A., Barthet-Barateig, A., Parker, H.N., Khurshid, A., Tessier, S., Sicard, M., Knox, A.J., Pang, L., and De Moor, C.H. (2012). Inhibition of polyadenylation reduces inflammatory gene induction. *RNA* 18, 2236–2250.
71. Alcobia, D.C., Ziegler, A.I., Kondrashov, A., Comeo, E., Mistry, S., Kellam, B., Chang, A., Woolard, J., Hill, S.J., and Sloan, E.K. (2018). Visualizing Ligand Binding to a GPCR In Vivo Using NanoBRET. *iScience* 6, 280–288.
72. Mali, P., Yang, L., Esvelt, K.M., Aach, J., Guell, M., DiCarlo, J.E., Norville, J.E., and Church, G.M. (2013). RNA-guided human genome engineering via Cas9. *Science* 339, 823–826.
73. Gibson, D.G., Young, L., Chuang, R.Y., Venter, J.C., Hutchison, C.A., 3rd, and Smith, H.O. (2009). Enzymatic assembly of DNA molecules up to several hundred kilobases. *Nat. Methods* 6, 343–345.
74. Klarenbeek, J.B., Goedhart, J., Hink, M.A., Gadella, T.W., and Jalink, K. (2011). A mTurquoise-based cAMP sensor for both FLIM and ratiometric read-out has improved dynamic range. *PLoS One* 6, e19170.